Lactate-depleted pillar[5]arene-based chiral supramolecular nanovesicles for L-glucose-mediated tumor-specific chemodynamic- and photodynamic- synergistic therapy

Zefan Zhang,[a,†] Wenyuan Cheng,[a,†] Hui Li,[b] Xinxin Li,[a] Xuan Zhang,[a] Yu Li,[c] and Baodui Wang*[a]

[a] Z. Zhang, W. Cheng, H. Li, X. Li, X. Zhang, Prof. B. Wang, State Key Laboratory of Applied Organic Chemistry and Key Laboratory of Nonferrous Metal Chemistry and Resources Utilization of Gansu Province, Lanzho University, Lanzhou, 730000, P. R. China.

[b] H. Li, Department of Cardiovascular Medicine, Affiliated Hospital of Yan'an University, Yan'an, 716000, P. R. China.

[c] Dr. Y. Li, Department of Magnetic Resonance, The First Clinical Medical College, Lanzhou University, Lanzhou, 730030, P.R. China.

[+] These authors contributed equally to this work.

E-mail: wangbd@lzu.edu.cn

Experimental section

Materials and Instruments. All commercially available compounds were used without further purification unless otherwise noted. All other reagents and solvents were commercially available at analytical grade and were used without further purification. transmission electron microscope (FEI，talos F200s(200kV)), UV-vis absorbance measurements were recorded on Agilent Cary 5000 UV-vis-NIR. NMR spectrums were gathered on a JEOL ESC 400 M instrument. Chemical shifts are reported in ppm downfield from tetramethylsilane (TMS, δ scale with solvent resonances as internal standards). Mass spectra were performed on a Bruker Esquire 3000 plus mass spectrometer (Bruker-Franzen Analytik GmbH Bremen, Germany) equipped with ESI interface and ion trap analyzer. Fluorescence microscopic images were obtained with a microscope (Olympus IX53 and Nikon eclipse Ti2). Circular dichroism (CD) spectroscopy is used to study the optical properties of chiral host by Circular Dichroism Spectrometer (JASCO-J1500). Living imaging of the mice was performed at predetermined time points using the VISQUE In vivo Smart-LF (Vieworks, Korea).

Synthesis and characterizations of compounds CP5

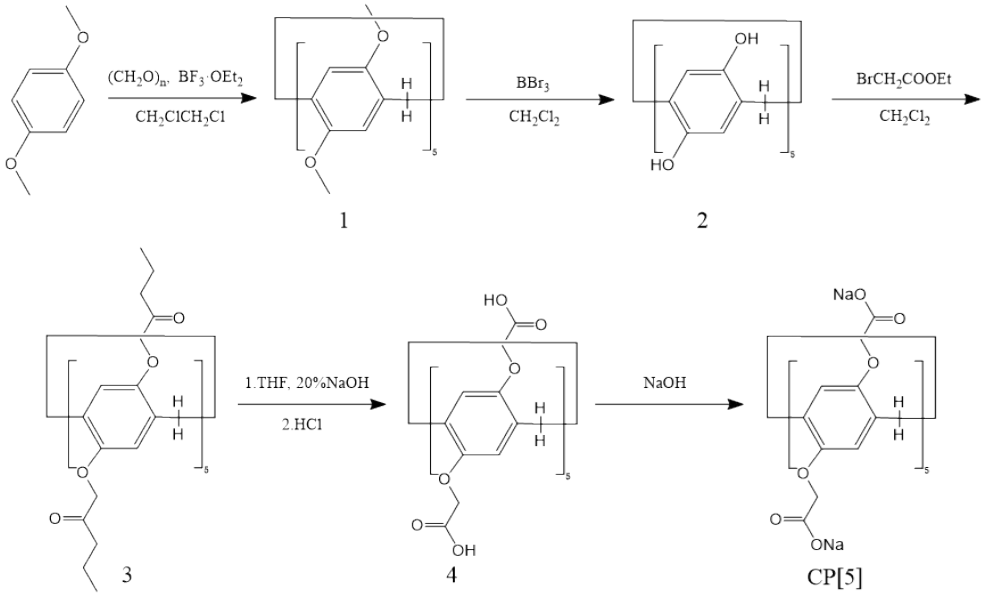

Scheme S1. Synthesis routes to the target compounds CP5.[1-3]

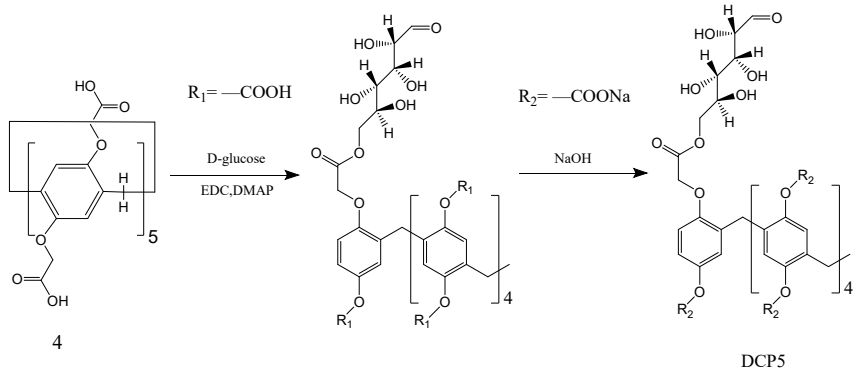

Scheme S2. Synthesis routes to the target compounds DCP5.

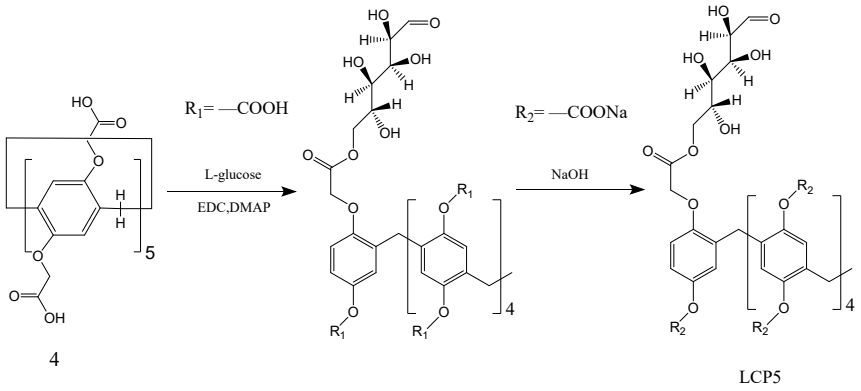

Scheme S3. Synthesis routes to the target compounds LCP5.

Synthesis and characterizations of compounds FeTPPNHC

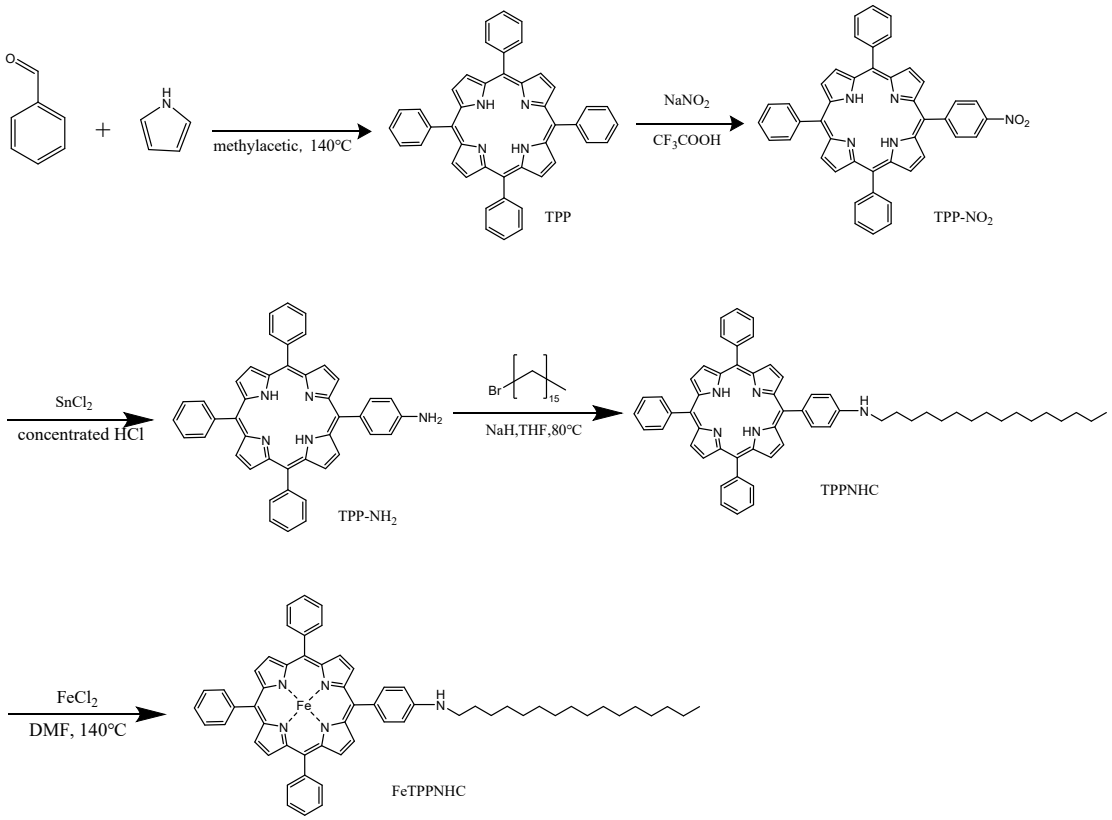

Scheme S4. Synthesis routes to the target compounds FeTPPNHC.

Synthesis of TPP: Freshly distilled pyrrole (56 ml, 0.8 mole) and 80 ml (0.8 mole) of reagent grade benzaldehyde are added to 3 1. of refluxing reagent grade propionic acid. (Note: crystalline material is not directly obtained if acetic acid is used.) After refluxing for 30 min, the solution is cooled to room temperature and filtered, and the filter cake is washed thoroughly with methanol. After a hot water wash, the resulting purple crystals are air dried, and finally dried in vacuo to remove adsorbed acid to yield 25 g (20 % yield) of TPP. (Note that longer reaction times in propionic acid do not appreciably improve the yield, but decrease the purity of the products.) ^{1}H NMR (400 MHz, Chloroform-d, 298 K): δ 8.88 (s, 8H), 8.27-8.23 (m, 8H), 7.80-7.75 (m, 12H), -2.72 (s, 2H).

Synthesis of TPP-NO_2: To a solution of TPP (1 g, 1.63 mmol) in TFA (50 mL) was added sodium nitrite (200 mg, 2.9 mmol). After 3 min stirring at room temperature, the reaction mixture was poured into water (500 mL) and extracted with dichloromethane (3×250 mL). The organic layer was washed with saturated aqueous $NaHCO_3$ and water as described above and then the solvent was removed under vacuum. The residue was further purified by silica gel

column chromatography (CH_2Cl_2：PE=1：1) to give TPP-NO_2. ^{1}H NMR (400 MHz, Chloroform-d, 298 K): δ 8.92 – 8.84 (m, 6H), 8.74 (d, J = 4.8 Hz, 2H), 8.64 (d, J = 8.5 Hz, 2H), 8.40 (d, J = 8.4 Hz, 2H), 8.21 (d, J = 6.7 Hz, 6H), 7.81-7.74 (m, 9H), -2.78 (s, 2H).

Synthesis of TPP-NH_2: Dissolve 0.8 g of TPP-NO_2 in 100 mL of concentrated HCl, and slowly add $SnCl_2$ (2.2 g, 0.975 mol) while stirring. Heat the solution to 65 °C, then reflux under an argon atmosphere for 1 hour. Subsequently, pour the solution into ice water to quench the reaction. Extract the mixture with CH_2Cl_2 (4×100 mL), followed by washing three times with 100 mL of water each. Finally, wash the organic phase with saturated $NaHCO_3$ solution until no bubbles are observed. Purify the product by silica gel column chromatography (CH_2Cl_2 : PE =3:1) to obtain pure TPP-NH_2.^{1}H NMR (400 MHz, Chloroform-d) δ 8.93 (d, J = 4.7 Hz, 2H), 8.83 (d, J = 2.5 Hz, 6H), 8.26 – 8.17 (m, 6H), 7.99 (d, J = 7.9 Hz, 2H), 7.80 – 7.70 (m, 9H), 7.08 – 7.02 (m, 2H), 4.02 (s, 2H), -2.75 (s, 2H).

Synthesis of TPPNHC: Dissolve TPP-NH_2 (0.629 g, 1 mmol) in 30 mL of tetrahydrofuran, and add NaH (0.096 g, 4 mmol) followed by stirring for 15 minutes. Then, add 0.38 g of 1-bromohexadecane to the mixture and heat to 80 °C under reflux for 24 hours. Quench the reaction by adding water and extract the mixture three times with CH_2Cl_2 (3×50 mL). Finally, purify the product by silica gel column chromatography to obtain pure **TPPNHC**. ^{1}H NMR (400 MHz, Chloroform-d) δ 8.98 (d, J = 4.7 Hz, 2H), 8.83 (d, J = 3.4 Hz, 6H), 8.22 (dt, J = 7.9, 2.2 Hz, 6H), 8.02 (d, J = 8.2 Hz, 2H), 7.79 – 7.71 (m, 9H), 6.98 (d, J = 8.3 Hz, 2H), 4.09 (s, 1H), 3.38 (t, J = 7.1 Hz, 2H), 1.82 (p, J = 7.2 Hz, 2H), 1.55 (d, J = 7.7 Hz, 2H), 1.28 (dd, J = 12.9, 5.8 Hz, 24H), 0.89 (s, 3H), -2.73 (s, 2H).

Synthesis of FeTPPNHC: Dissolve TPPNHC (0.17 g, 0.2 mmol) in 20 mL of DMF, and add 0.5 g of $FeCl_2 \cdot H_2O$ with stirring until complete dissolution. React the mixture at 140 °C in an oil bath for 6 hours, then pour the solution into 100 mL of H_2O. Separate the water-insoluble precipitate by centrifugation, and wash it three times with 1 M of HCl and H_2O, respectively. Finally, dissolve the product in CH_2Cl_2, wash the organic phase twice with H_2O, and evaporate the solvent to dryness to obtain FeTPPNHC. The coordination of FeTPPNHC was characterized by comparative analysis using nuclear magnetic resonance spectroscopy.

Synthesis of LOx@LCP5⊃FeTPPNHC: First, mix a 500 μM DMSO solution of FeTPPNHC and a 50 μM aqueous solution of LCP5 in a volume ratio of 1:10, and shake the

mixture for 10 minutes. Subsequently, freeze the sample using liquid nitrogen and lyophilize it to remove DMSO and H2O, yielding a 1:1 complex of LCP⊃FeTPPNHC. Dissolve the complex in water by sonication, add LOx at a concentration of 2 U/mL, and sonicate for an additional 30 seconds to obtain a green solution to obtain LOx@LCP5⊃FeTPPNHC. LOx@CP5⊃FeTPPNHC and LOx@DCP5⊃FeTPPNHC are synthesised by same way. Finally, characterize the morphology and size of the assembly using transmission electron microscopy .

NMR Titration for Host-Guest Interaction Studies

Dissolve 4 mg of TPPNHC in 0.6 mL of Chloroform-d. Subsequently, add 2.2 mg of methylated pillar[5]arene (compound 1 in Figure S1, MP5) to the solution in four separate aliquots, resulting in molar concentration ratios of TPPNHC to MP5 of 2:1, 2:2, 2:3, and 2:4, respectively. After each addition of MP5, perform adn compare ^{1}H NMR spectroscopy to characterize the host-guest interactions.

UV-Vis Titration for Guest Variation Studies

Dissolve 1.2 mg of FeTPPNHC in 0.5 mL of DMF, and dissolve 3.9 mg of LCP5 in 1 mL of H_2O. Add 10 μL of the FeTPPNHC solution, followed by 2 μL of the LCP5 aqueous solution, and dilute the mixture with water to a final volume of 2.5 mL to achieve a molar ratio of 5:1 (FeTPPNHC:LCP5). While keeping the concentration of FeTPPNHC constant (10^{-5} M), prepare solutions with varying molar ratios of FeTPPNHC:LCP5 , such as 5:1, 5:2, 5:3, 5:4, 5:5, 5:6, 5:7, 5:8, and 5:9. Measure the characteristic absorption spectra of FeTPPNHC in these solutions using a UV-vis-NIR spectrophotometer.

Fluorescence Titration for Host Variation Studies

Dissolve 1.2 mg of FeTPPNHC in 0.5 mL of DMF, and dissolve 3.9 mg of LCP5 in 1 mL of H_2O. Using a pipette, add 10 μL of the LCP5 solution, followed by 2 μL of the FeTPPNHC solution, and dilute the mixture with water to a final volume of 2.5 mL to achieve a molar ratio of 1:5 (FeTPPNHC:LCP5). While keeping the concentration of LCP5 constant (10^{-5} M), prepare solutions with varying molar ratios of FeTPPNHC:LCP5 , such as 1:5, 2:5, 3:5, 4:5, 5:5, 6:5, 7:5, 8:5, and 9:5, using the same method. Measure the characteristic fluorescence emission spectra of LCP5 in these solutions using a fluorescence spectrophotometer.

Job's Method for Determining the Optimal Complexation Ratio

Prepare stock solutions of FeTPPNHC and LCP5 as well as Fluorescence Titration. Take 10 test tubes and add 2, 4, 6, 8, 10, 12, 14, 16, 18, and 20 μL of the FeTPPNHC solution to each tube, respectively. Then, add 20, 18, 16, 14, 12, 10, 8, 6, 4, and 2 μL of the LCP5 solution to the corresponding tubes. Dilute each mixture with water to a final volume of 2.5 mL, resulting in mixed solutions with a total concentration of 20 μM and varying molar ratios of FeTPPNHC to LCP5. Measure the characteristic absorption spectra of FeTPPNHC in these solutions using a UV-vis-NIR spectrophotometer. Plot the relative intensity of the characteristic absorption of FeTPPNHC at 412 nm against the molar fraction of FeTPPNHC to determine the optimal complexation ratio.

Critical Micelle Concentration (CMC) Measurement

Prepare a 10^{-6} M aqueous solution of pyrene (analytical standard). Using this solution, prepare a series of solutions with a 1:1 complexation ratio of LCP5⊃FeTPPNHC at concentrations of 5, 10, 15, 20, 30, 40, 50, 60, 70, 80, and 100 μM. Measure the fluorescence emission spectra of pyrene at two characteristic wavelengths using a fluorescence spectrophotometer. Calculate the ratio of the fluorescence intensities (I_1/I_3) at these two wavelengths and plot it against the logarithm of the concentration. Fit the data to determine the critical micelle concentration (CMC) of LCP5⊃FeTPPNHC.

Lactate Oxidase (LOx) Standard Curve

Dissolve 1000 U of LOx in 1 mL of PBS (pH 7.4) to prepare a stock solution. Dilute the stock solution to obtain LOx solutions at different concentrations (in U/mL). Measure the characteristic UV absorbance of each solution using a UV-vis spectrophotometer. Plot the UV absorbance against the LOx concentration and fit the data to establish the LOx standard curve.

LOx Encapsulation Efficiency and pH-dependent Release Capability

LOx Encapsulation Efficiency (EE) Calculation: Measure the UV-vis-NIR spectra of 80 μM LCP5⊃FeTPPNHC and LOx@LCP5⊃FeTPPNHC. Calculate the change in absorbance at the characteristic UV absorption wavelength and use the LOx standard curve to determine the concentration of dispersed LOx in the solution. Calculate the encapsulation efficiency (EE) using the formula:

$$EE(\%)=1-(M_{so}/M_{added})\times 100\%.$$

where *Mso* is the mass of LOx in the supernatant and Madded is the total mass of LOx added.

Acid-Responsive Performance Verification: Measure the UV-vis-NIR spectra of LOx@LCP5⊃FeTPPNHC at pH 5.5 and compare it with the spectra obtained under neutral conditions (pH 7.4) to verify its acid-responsive behavior.

Morphological Characterization: Use transmission electron microscopy (TEM) to characterize the morphology of LOx@LCP5⊃FeTPPNHC under both pH 5.5 and neutral conditions (pH 7.4).

Consume Capability of GSH

Standard Curve of GSH: Configure 10 mM solution of GSH and 7.5 mg/ml solution of DTNB. Take appropriate amount of GSH mother liquor and configure different concentration solution of GSH in 2.5 ml(0.024, 0.036, 0.04, 0.052, 0.06 mM), then measure the UV-vis-NIR spectra of these solution after adding 10 μl solution of DTNB for 30 min, Plot the standard curve of GSH from absorbance in 412 nm and concentration.

Calculation of GSH Consumption: Incubate the 80 μM LCP5⊃FeTPPNHC in about 20 mM GSH solution, add 10 μl of the GSH solution to 2.5 ml PBS(pH 7.4) after incubating for 0, 12, and 24h respectively. Then add 10 μl of 12 mg/ml DTNB solution to these mixture and incubate for 30 min. Measure the UV-vis-NIR spectra of these solution and use the GSH standard curve to calculate the concentration and variation of GSH.

Cell Culture

MCF cells were cultured in an environment of 21% O_2, 5% CO_2, and 74% N_2 at 37°C in an incubator. Once the cells reached 90% confluence, they were passaged. Cells from the second passage were used for subsequent experiments.

In Vitro Cytotoxicity Assay

The cytotoxicity of LOx@LCP5⊃TPPNHC against MCF-7 and NIH3T3 cells was evaluated using the CCK-8 assay. MCF-7 cells were cultured in 96-well plates until reaching an appropriate density. Subsequently, PBS solutions containing LOx@LCP5⊃TPPNHC at concentrations of 400, 200, 100, 50, 25, 12.5, 6.25, and 3.13 μM were added to the wells, followed by incubation for 24 hours. Finally, CCK-8 solution was added, and the absorbance was measured using a microplate reader to calculate the survival rate of MCF-7 cells.

Cellular Uptake Measurement

MCF-7 Cells were first cultured in a medium containing the drug at a concentration of 10 μM. Subsequently, the cell nuclei were stained with DAPI for localization, and the uptake of LOx@LCP5⊃FeTPPNHC, LOx@DCP5⊃FeTPPNHC, and LOx@CP5⊃FeTPPNHC by tumor cells at the same time point was characterized using an inverted fluorescence microscope.

Intracellular ROS detection

Intracellular ROS levels were measured using DCFH-DA. MCF-7 cells were first incubated in 24-well plates until reaching an appropriate density. Subsequently, the cells were treated with 10 μM LOx@LCP5⊃FeTPPNHC supramolecular PBS solution in the dark for 1 hour. The original medium was then replaced with 11 μM DCFH-DA staining solution and incubated for 30 minutes. Finally, one well was irradiated with a laser (660 nm, 400 mW/cm²) for 10 minutes, and both irradiated and non-irradiated groups were imaged using an inverted fluorescence microscope. The same procedure was applied to image cells treated with achiral vesicles (LOx@CP5⊃FeTPPNHC) and D-type vesicles (LOx@LCP5⊃FeTPPNHC).

Measurement of Synergistic Therapeutic Efficacy

MCF-7 cells were cultured in two 96-well plates until reaching an appropriate density. PBS solutions containing LOx@LCP5⊃FeTPPNHC at concentrations of 100, 50, 25, 12.5, 6.25, 3.13, 1.56, 0.75, and 0.33 μM were added to each plate, followed by incubation for 1 hour. The cells were then cultured in normal medium and irradiated with a 660 nm laser (400 mW/cm²) for 10 minutes, followed by further incubation for 24 hours. Finally, CCK-8 solution was added, and the absorbance was measured using a microplate reader to calculate the cell survival rate. For the second 96-well plate, the same treatment was applied without laser irradiation, and the tumor cell survival rate was calculated after 24 hours. The same method was used to evaluate the cytotoxicity of different control groups, including LCP5⊃FeTPPNHC + Laser, LOx@LCP5⊃TPPNHC + Laser, and LOx@LCP5⊃FeTPPNHC in the dark, at the same concentrations.

Investigetion of effect to chiral-glucose-mediation on cytotoxicity

The cytotoxicity of LOx@LCP5⊃FeTPPNHC, LOx@DCP5⊃FeTPPNHC, and LOx@CP5⊃FeTPPNHC with different chiral vesicles against cells was measured using the aforementioned CCK-8 assay as same as measurement of synergistic therapeutic efficacy except the concentrations(3.125, 6.25, 12.5, 25, 50, 100, 200, 400, 800 μM).

Animals

Balb/c mice were obtained from the Animal Experiment Center of the Lanzhou Veterinary Research Institute. All mice were female, aged 6-7 weeks, and all animal experiments were conducted in accordance with the safety practice guidelines approved by the Ethics Committee for Human Specimens and Animal Experiments of the Basic Medical College of Lanzhou University. A total of 100 μL of 2×10^5 4T1 cells dispersed in PBS was subcutaneously injected into the right hind leg of each mouse. The mice were then cultured for 9 days to establish a breast cancer tumor-bearing mouse model. All animal experiments were performed according to the Guidelines for Safe Work Practices approved by the Committee on Ethics of Human Specimens and Animal Experiments at College of Chemistry and Chemical Engineering, Lanzhou University (2023004).

Animals In vivo biodistribution and metabolize evaluation

The breast cancer mouse model was divided into 7 groups, with 5 mice in each group. Using FeTPPNHC as the quality standard, a LOx@LCP5⊃FeTPPNHC solution with a LOx concentration of 1 U/mL was prepared. Each mouse was administered the solution at a dose of 5 mg/kg every 2 days. Five hours after each administration, the tumor area of the mice was irradiated with a 660 nm laser at 400 mW/cm² for 5 minutes. On the 15th day of treatment, the mice were dissected, and the size of the tumor tissues was compared. Using the same administration and treatment protocol, the therapeutic effects were evaluated for the following groups: PBS, LOx@LCP5⊃FeTPPNHC, LOx@DCP5⊃FeTPPNHC, LOx@CP5⊃FeTPPNHC, LOx@LCP5⊃TPPNHC, LCP5⊃FeTPPNHC (6 irradiated groups), and LOx@LCP5⊃FeTPPNHC (non-irradiated group).

H&E staining

For evaluating the pathological damages to tumors of different treatments, the tumor tissues in each group were retrieved after the 15 days of treatment and processed for H&E staining analysis.

In Vivo Fluorescence Imaging

To avoid the interference of food on fluorescence imaging, tumor-bearing mice of similar tumor size were fasted for 12 hours. Subsequently, the mice were administered the drug at a concentration of 10 mg/kg. In vivo fluorescence analysis of the liver, kidney, and tumor regions

was performed at 0, 1, 3, 5, 6, 7, and 9 hours post-administration. This was conducted to evaluate the metabolic process and targeting efficiency of LOx@LCP5⊃FeTPPNHC.

Investigation on the Targeting Performance of Chiral Vesicles In Vivo

Using the aforementioned method, mice were treated and administered with different chiral vesicles (LOx@LCP5⊃FeTPPNHC, LOx@DCP5⊃FeTPPNHC, and LOx@CP5⊃FeTPPNHC). Fluorescence imaging of the mice was performed 5 hours post-administration, and the relative fluorescence intensity of symmetrical regions in the same mouse was analyzed. This approach was used to compare the targeting performance of different chiral vesicles in vivo.

Hematoxylin and Eosin (H&E) Staining

To evaluate the pathological damage to tumors caused by different treatment methods, mice were dissected 15 days after treatment, and tumor tissues from each group were collected for H&E staining analysis. Additionally, to assess the physiological changes in mice treated with LOx@LCP5⊃FeTPPNHC + Laser irradiation, major organs (heart, liver, spleen, lungs, and kidneys) were excised for morphological observation and subjected to H&E staining analysis.

Inhibition of Tumor Metastasis

Four groups of mice were treated in vivo with LOx@LCP5⊃FeTPPNHC, LOx@DCP5⊃FeTPPNHC, LOx@CP5⊃FeTPPNHC, and PBS, respectively, followed by laser irradiation. The treatment continued for nearly 30 days until the tumor size in the PBS group reached approximately 18 mm. The mice were then dissected to observe the morphology of the heart, liver, spleen, lungs, and kidneys, as well as the size of the corresponding tumors. The effectiveness of inhibiting tumor metastasis was assessed through H&E staining of the major organs and tumors.

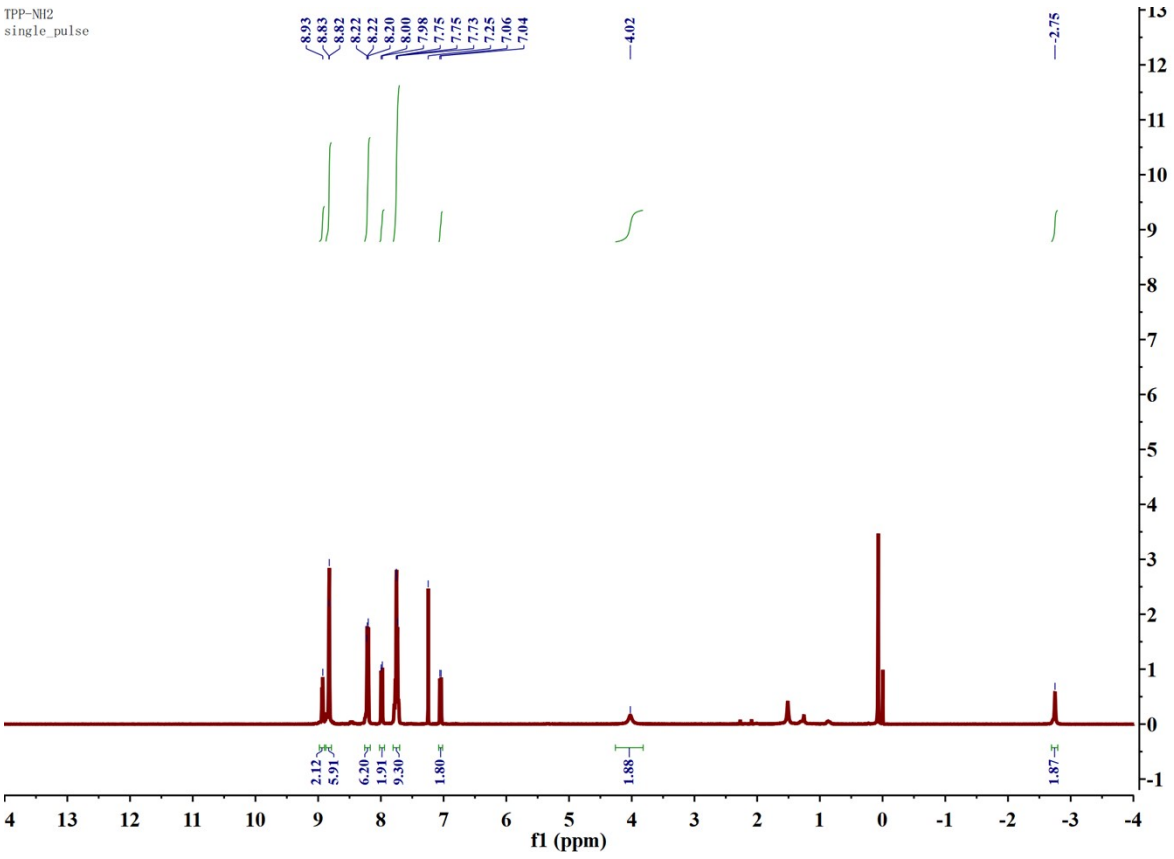

Figure S1. ^{1}H NMR spectrum (400 MHz, Chloroform-d, 298 K) of **TPP-NH$_2$**.

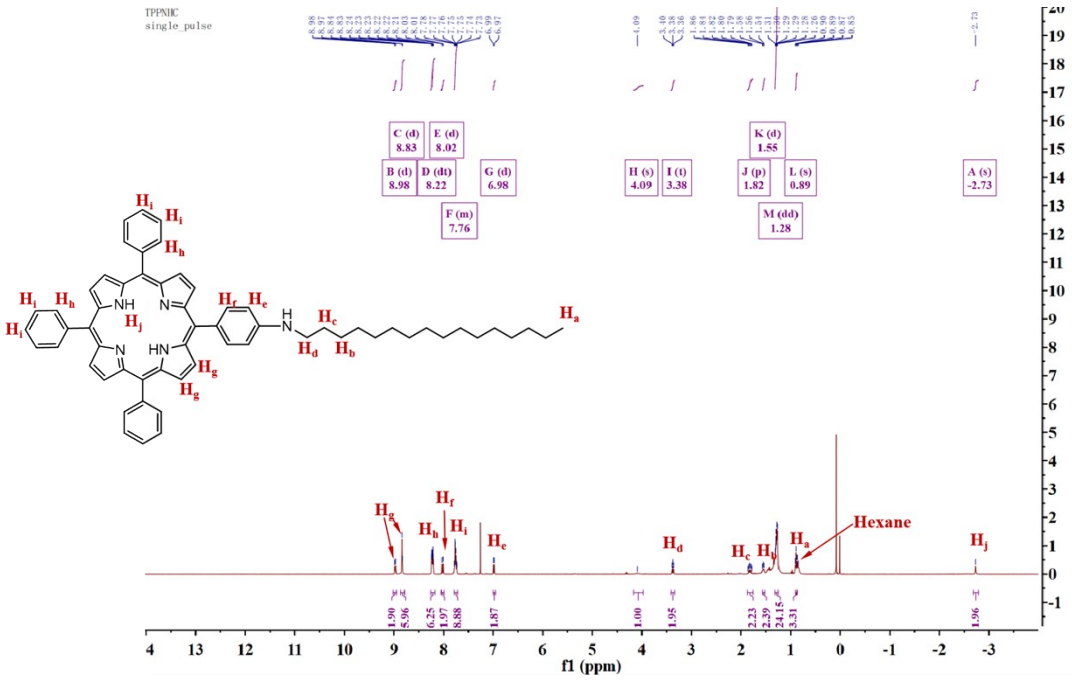

Figure S2. ^{1}H NMR spectrum (400 MHz, Chloroform-d, 298 K) of **TPPNHC**.

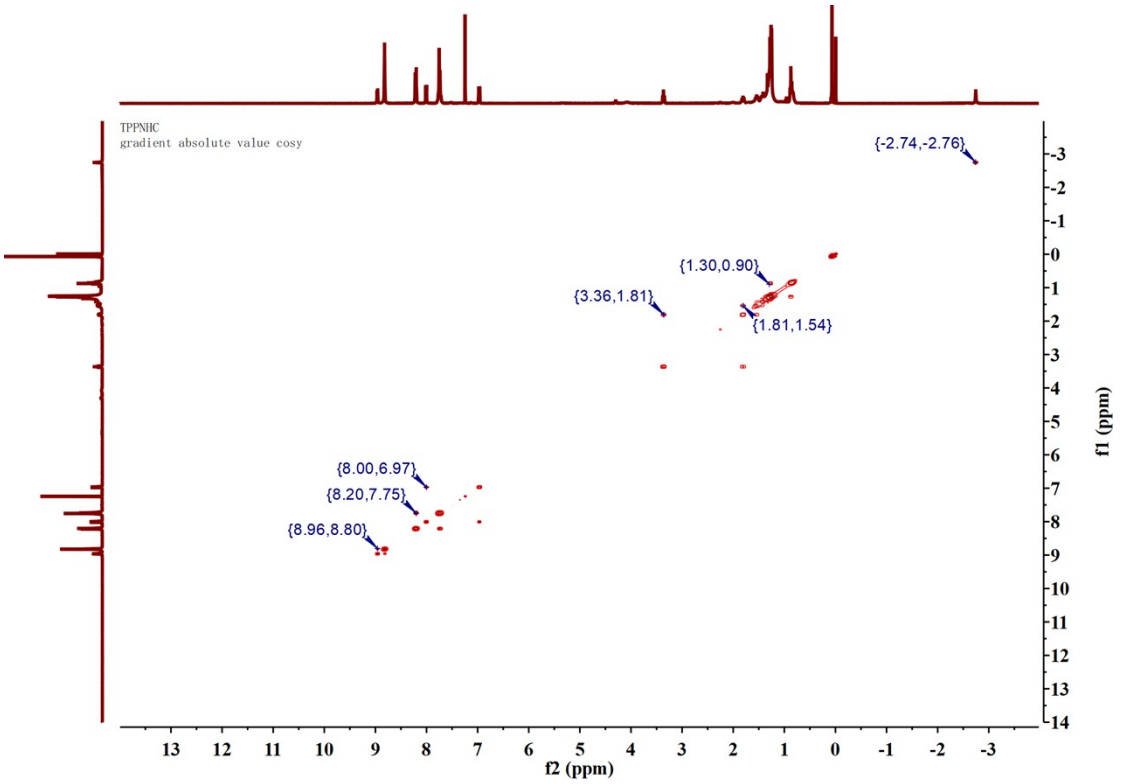

Figure S3. ^{1}H-^{1}H COSY spectrum (400 MHz, Chloroform-d, 298 K) of **TPPNHC**.

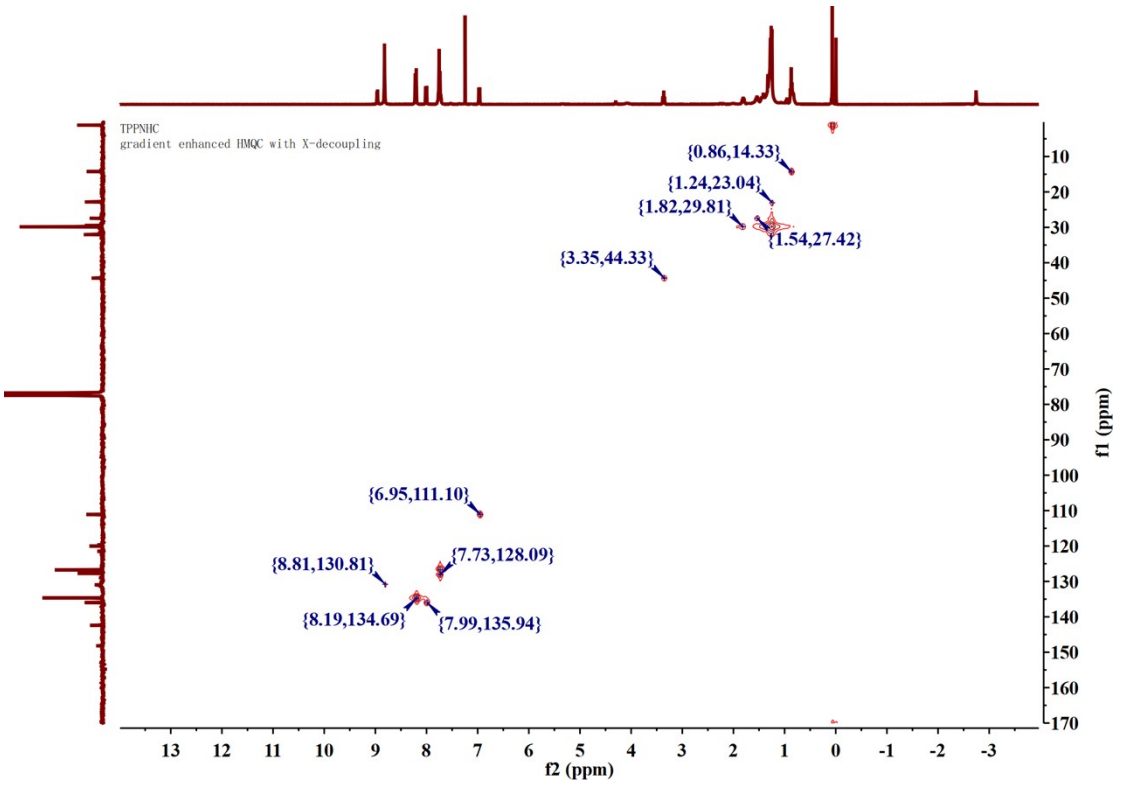

Figure S4. heteronuclear multiple quantum coherence ^{1}H-^{13}C NMR spectrum (400 MHz, $CDCl_3$, 298 K) of **TPPHNC**.

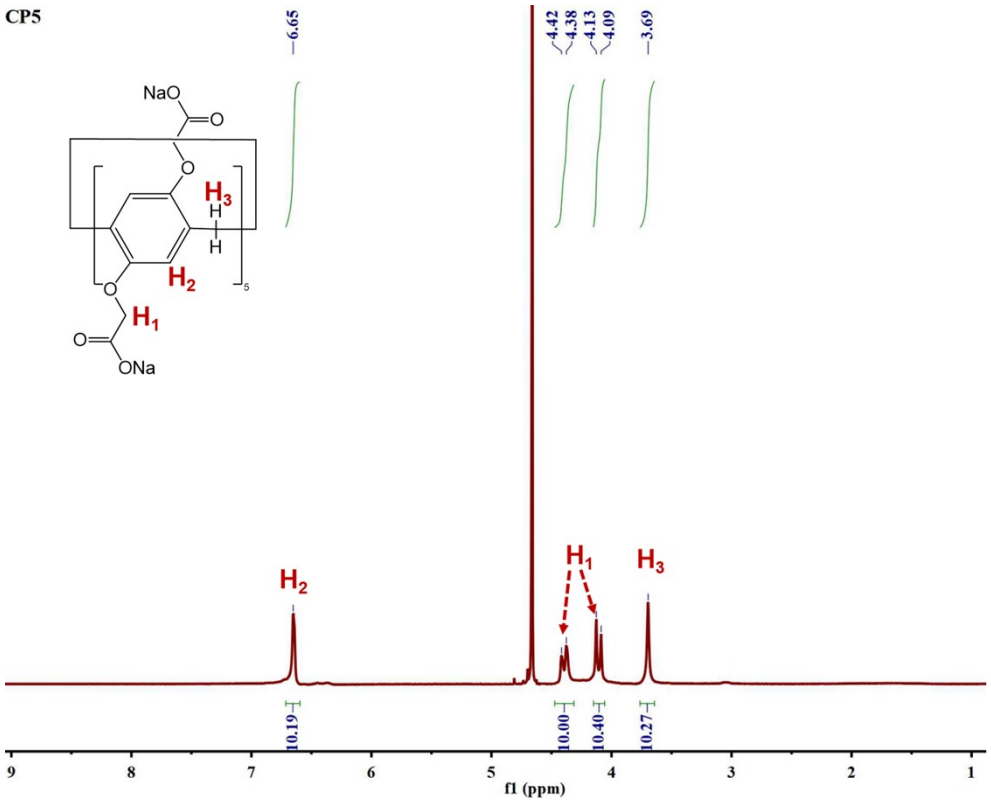

Figure S5. ^{1}H NMR of **CP5**(400 MHz, D_2O, 298 K)

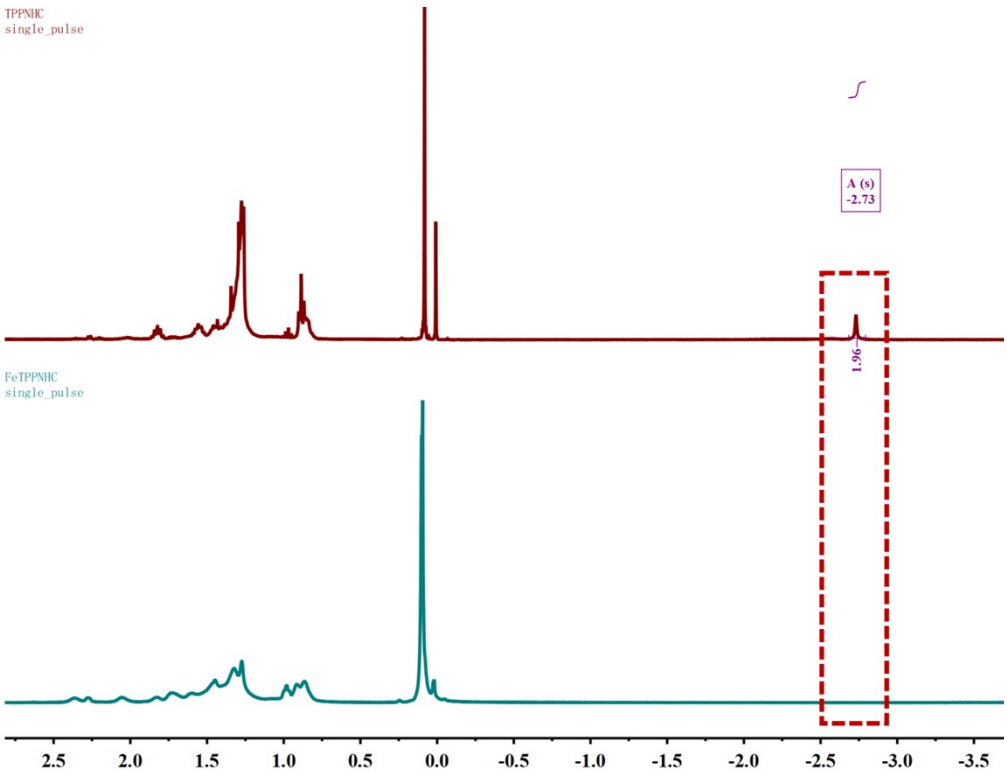

Figure S6. Comparison of ^{1}H NMR spectrum between **TPPHNC** and **FeTPPNHC** (400 MHz, $CDCl_3$, 298 K)

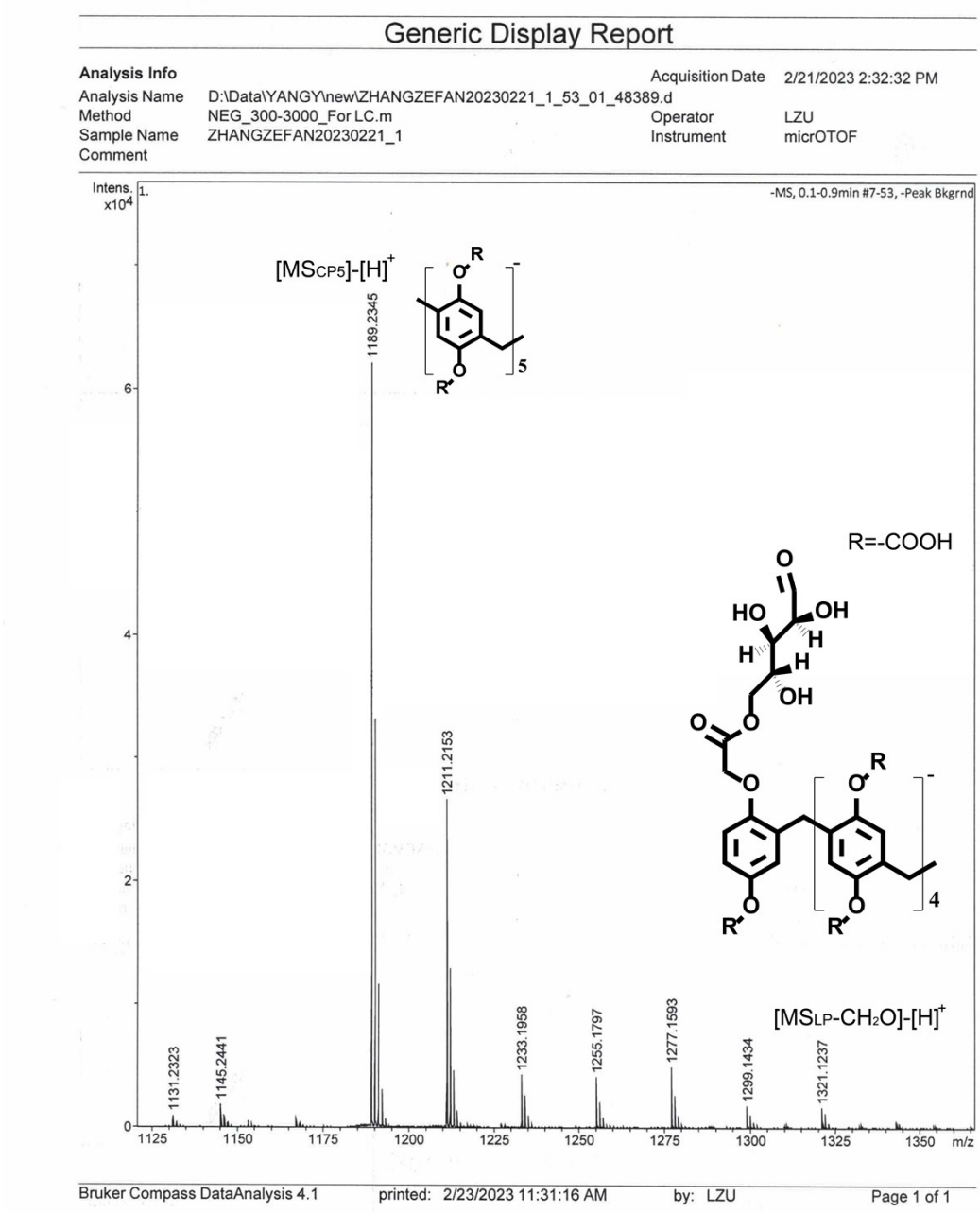

Figure S7. Electrospray ionization-mass spectrometry (ESI-MS)of **LCP5**.

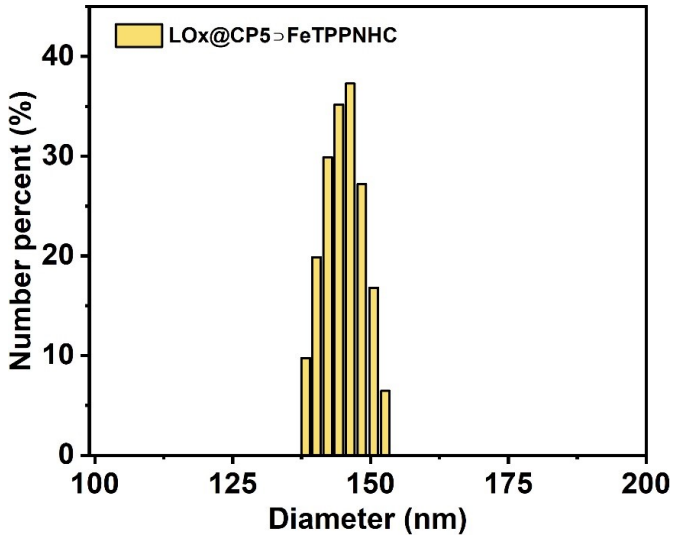

Figure S8. Average hydrodynamic diameters of LOx@CP5⊃FeTPPNHC

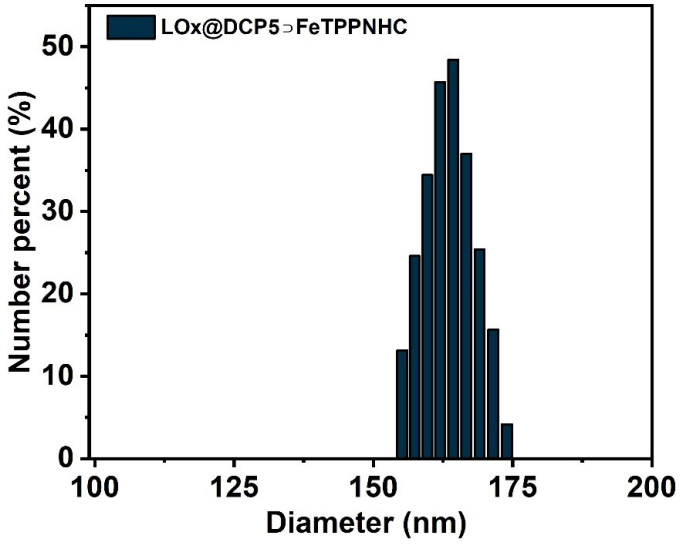

Figure S9. Average hydrodynamic diameters of LOx@DCP5⊃FeTPPNHC

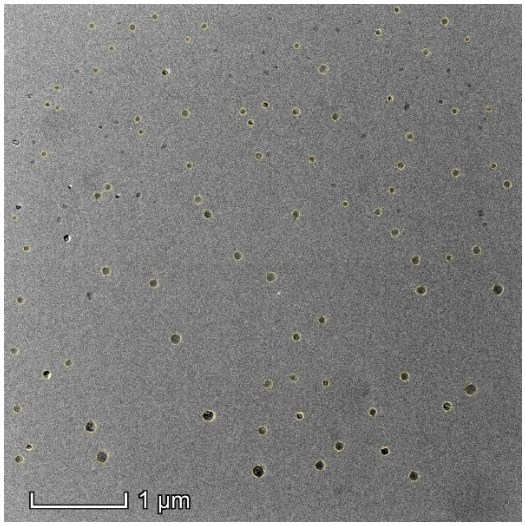

Figure S10. TEM imaging for estimating the size of LOx@LCP5⊃FeTPPNHC.

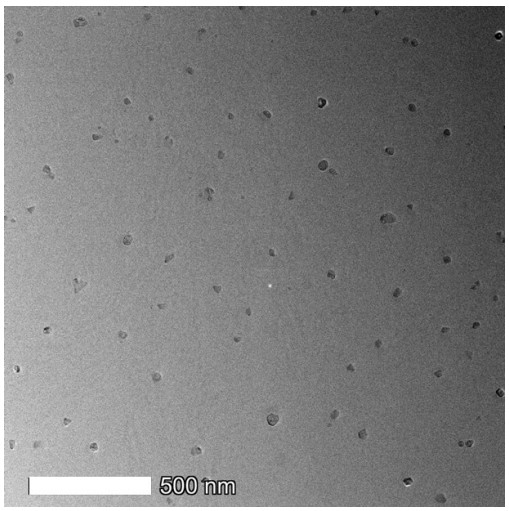

Figure S11. TEM imaging of LOx@DCP5⊃FeTPPNHC in PBS(pH=7.4).

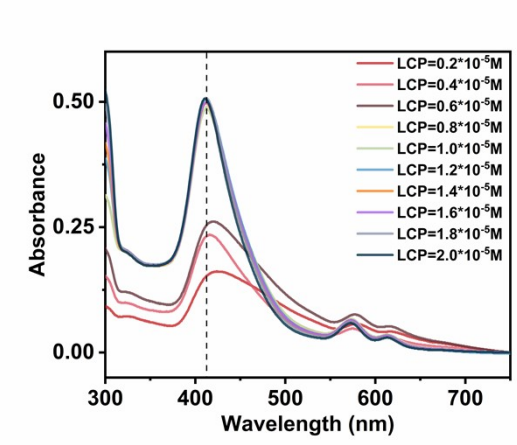

Figure S12. UV-vis-NIR Spectra of 10 μM FeTPPNHC solution

in different concentration of LCP5 solution(2, 4, 6, 8, 10, 12, 14, 16, 18, and 20μM).

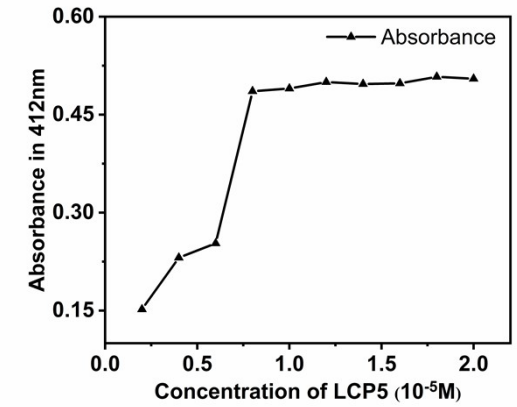

Figure S13. Plot of UV-vis-NIR Spectra of 10 μM FeTPPNHC solution

in different concentration of LCP5 solution(λ_{ob}=412nm)

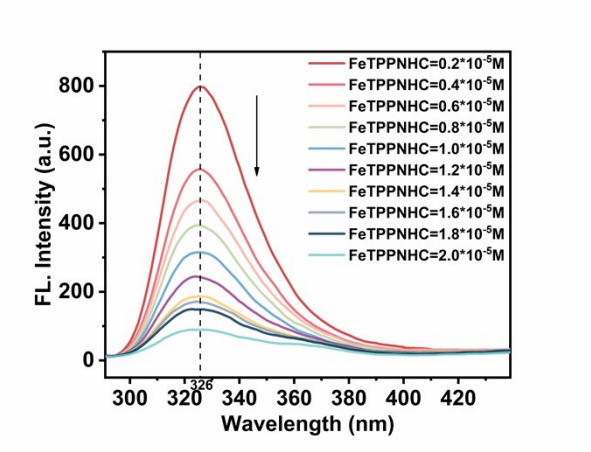

Figure S14. Fluorescence emission spectra of 10 μM LCP5 solution in different concentration of FeTPPNHC solution(2, 4, 6, 8, 10, 12, 14, 16, 18, and 20μM) (Ex: 240 nm, Em: 326 nm).

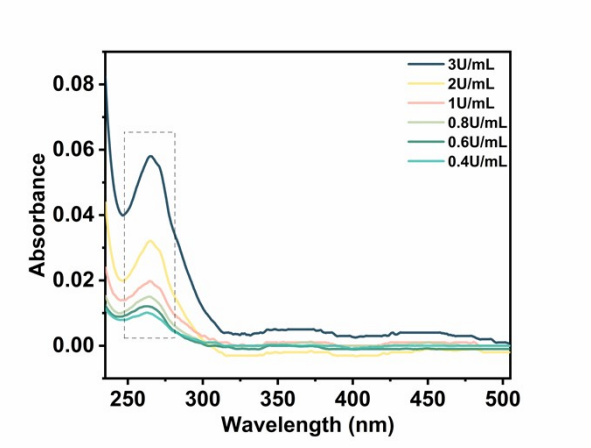

Figure S15a. UV-vis-NIR Spectra of LOx solution(0.4, 0.6, 0.8, 1, 2, and 3 U/ml).

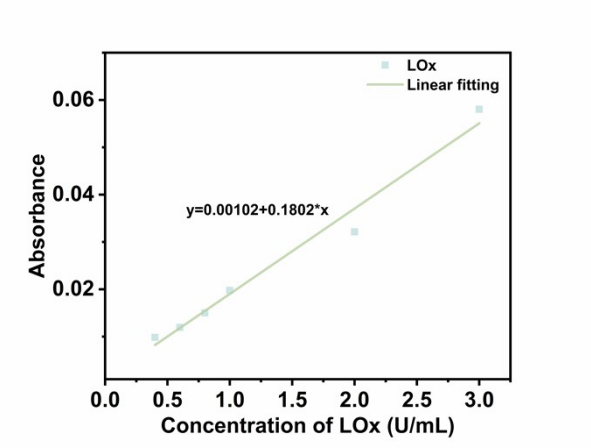

Figure S15b. UV absorbance standard curves of LOx.

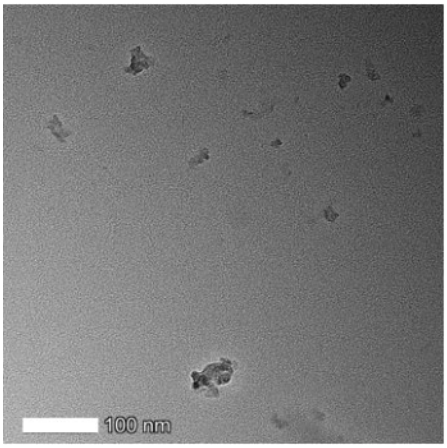

Figure S16. TEM imaging of **LOx@LCP5⊃FeTPPNHC** under acidic condition(pH=5.5).

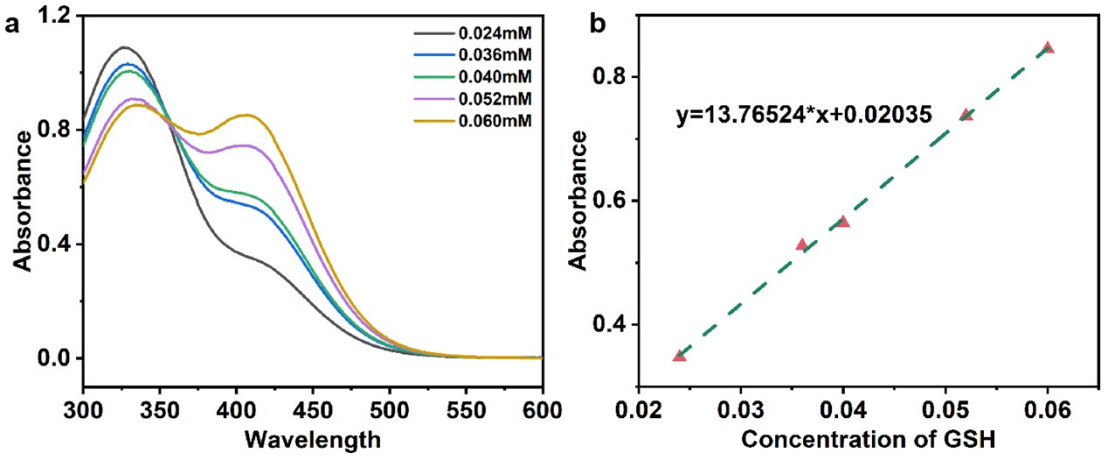

Figure S17 (a) the UV-vis absorbance of DTNB solution(0.03 mg/ml) at different concentration of GSH and (b) the standard curve of GSH concentration.

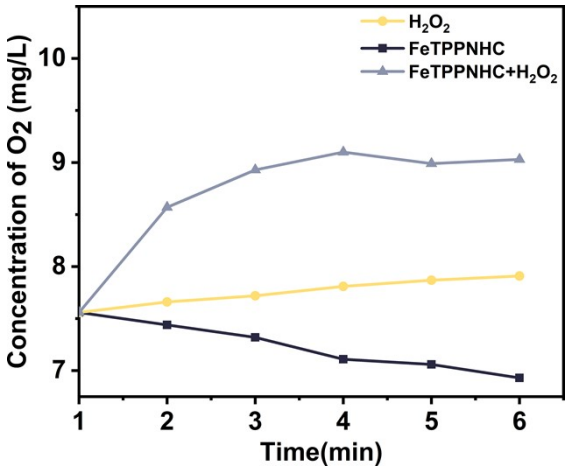

Figure S18. Dissolved oxygen in FeTPPNHC, 1mM H_2O_2, and FeTPPNHC+1mM H_2O_2 solutions.

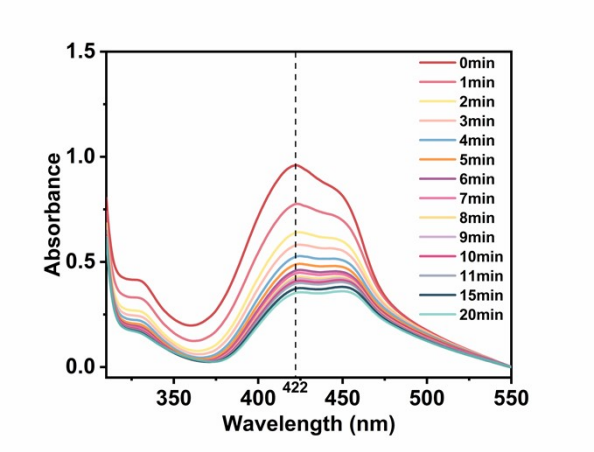

Figure S19. UV-vis absorbance of DPBF solution with LCP5⊃FeTPPNHC without H_2O_2 stimulated by red-laser for different time(660nm, 400mW/cm^2).

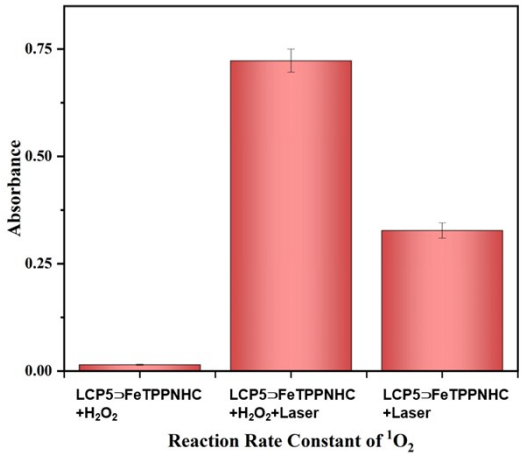

Figure S20. The Constants of reaction rate for $^1O_2$ under three different conditions(LCP5⊃FeTPPNHC+H_2O_2+Laser, LCP5⊃FeTPPNHC+Laser, and LCP5⊃TPPNHC+H_2O_2).

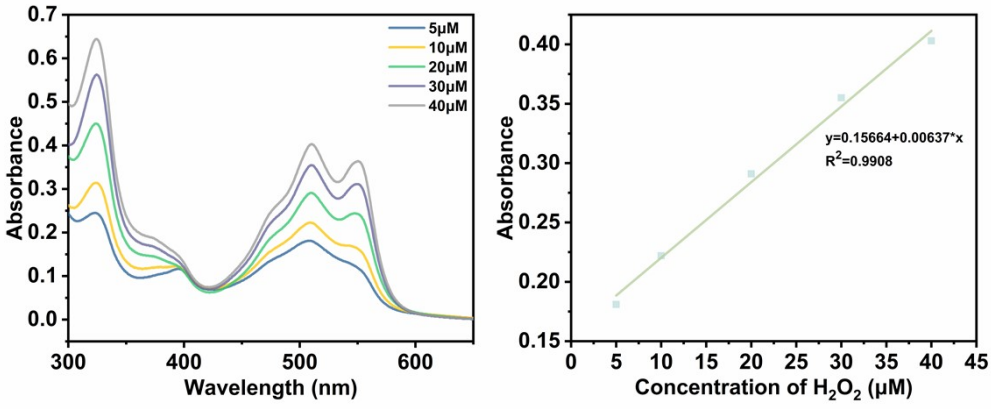

Figure S21. UV-vis spectra of DPD solution with in different concentration of H_2O_2 and standard curve of H_2O_2 versus concentration.

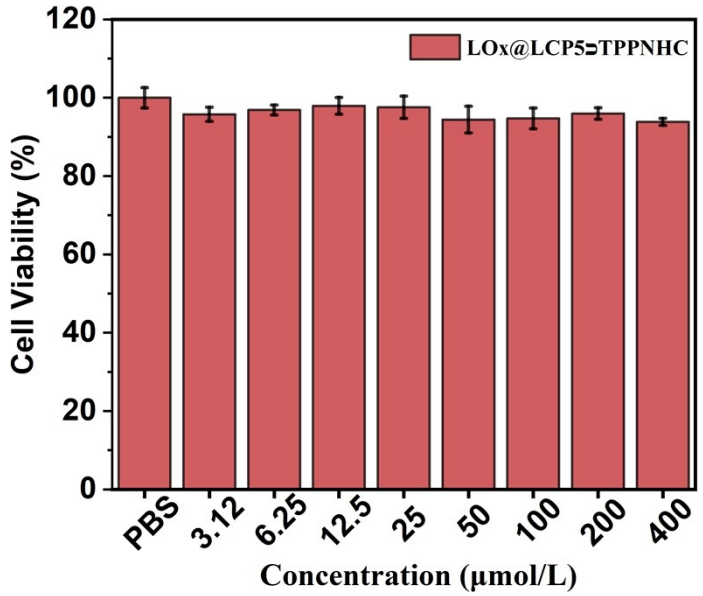

Figure S22. Cytotoxicity of LOx@LCP5⊃TPPNHC to MCF-7 cells.

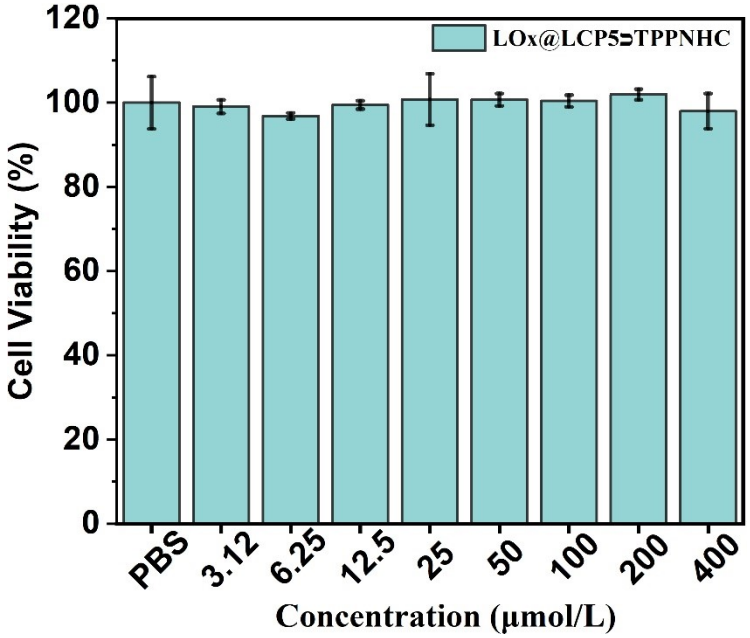

Figure S23. Cytotoxicity of LOx@LCP5⊃TPPNHC to NIH3T3 cells.

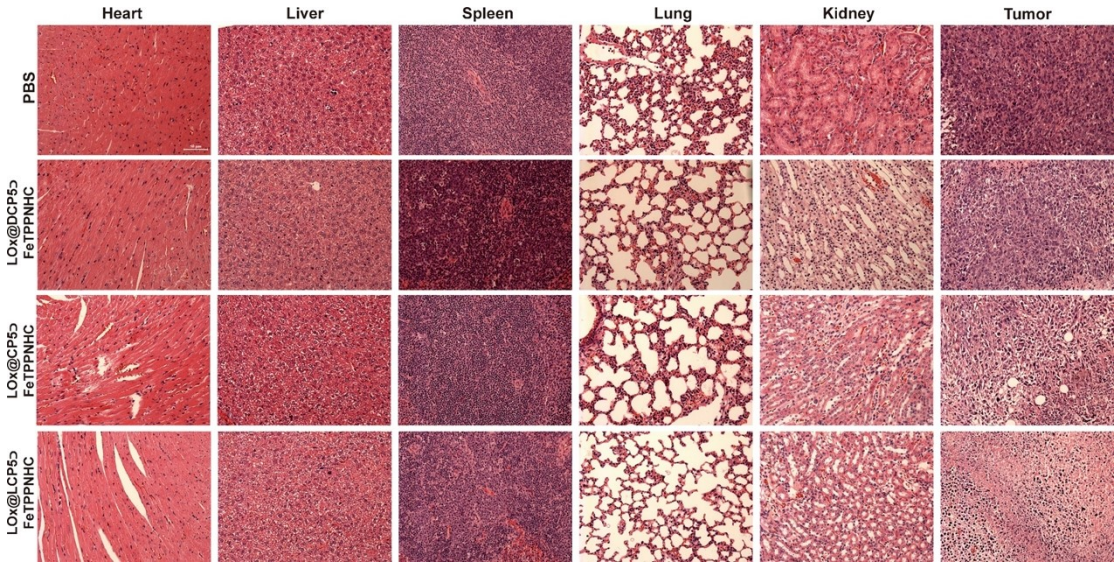

Figure S24. H&E staining images of the tumor sections of different treatment groups:PBS, LOx@LCP5⊃FeTPPNHC, LOx@DCP5⊃FeTPPNHC, LOx@CP5⊃FeTPPNHC, and PBS.

References

1. Ogoshi, T.; Yamagishi, T.-a.; Nakamoto, Y. *Chem. Rev*. **2016**, 116, 7937-8002.
2. Ogoshi, T.; Kakuta, T.; Yamagishi, T.-a. *Angew. Chem. Int. Ed*. **2019**, 58, 2197–2206.
3. Kakuta, T.; Yamagishi, T.-a.; Ogoshi, T. *Acc. Chem. Res*. **2018**, 51, 1656−1666.